J. Fluid Mech. (1996), *vol.* 312, *pp.* 125–148

Instabilities of the upstream meniscus in directional viscous fingering

By SYLVAIN MICHALLAND†, MARC RABAUD‡ AND YVES COUDER

Laboratoire de Physique Statistique de l'Ecole Normale Supérieure, 24 rue Lhomond, 75231 Paris Cedex 05, France

(Received 27 April 1995 and in revised form 10 November 1995)

New instabilities affecting the meniscus of a viscous fluid are presented. They occur in an experimental set-up introduced previously by Rabaud *et al.* (1990) in which a small quantity of a viscous fluid is placed in the narrow gap between two rotating cylinders. In this geometry the downstream meniscus located in the region where the two solid surfaces move away from each other is known to be unstable and to exhibit directional viscous fingering. In the present article it is shown that the upstream meniscus can also be unstable. Two types of instabilities are observed. In the first supercritical transition the front becomes time-dependent with either standing or propagating waves. In a second transition, which is subcritical, parallel fingers of finite amplitude are formed. The various types of spatio-temporal dynamical behaviour are discussed.

1. Introduction

Even though they are the simplest, one-dimensional spatially extended systems can still exhibit a large variety of dynamical behaviour. On the basis of symmetry arguments Coullet & Iooss (1990) predicted the existence of ten possible dynamical behaviours, some of which have not yet been observed. This is a motivation for seeking new one-dimensional instabilities. Experimentally this does not mean looking for instabilities in a one-dimensional medium, but simply studying instabilities which give rise to a series of structures (convection cells, vortices, fingers, etc....) in geometries such that the coupling and the dynamics of these structures can be considered as one-dimensional. This can be done in experiments such as the Rayleigh–Bénard instability (Daviaud, Bonnetti & Dubois 1990), when confined in narrow cells. But the main tool for the recent investigation of the dynamical regimes of one-dimensional extended systems has been the investigation of various types of interfacial fronts. When a front is globally stabilized by an external gradient, its instability generally leads to the formation of a cellular front. A review of these instabilities can be found in Flesselles, Simon & Libchaber (1991). Amongst such systems we can quote directional solidification (Jackson & Hunt 1965; Kurowski *et al.* 1989; Kurowski, de Cheveigné & Guthmann 1990), directional phase transition of liquid crystals (Oswald, Bechhoeffer & Libchaber 1987; Flesselles *et al.* 1991), the solidification front of eutectic alloys (Faivre *et al.* 1989), the front of a viscous fluid flowing down inside a rotating cylinder (Melo & Douady 1993), the destabilization of a falling liquid sheet (Limat *et al.* 1992) and directional viscous fingering (Taylor 1963; Hakim *et al.* 1990, Rabaud, Michalland

† Present Address: MFPM, Place des Carmes Déchaux, 63040 Clermont-Ferrand Cedex, France.
‡ Present Address: FAST, Bt. 502, 91405 Orsay Cedex, France (to where correspondence should be addressed).

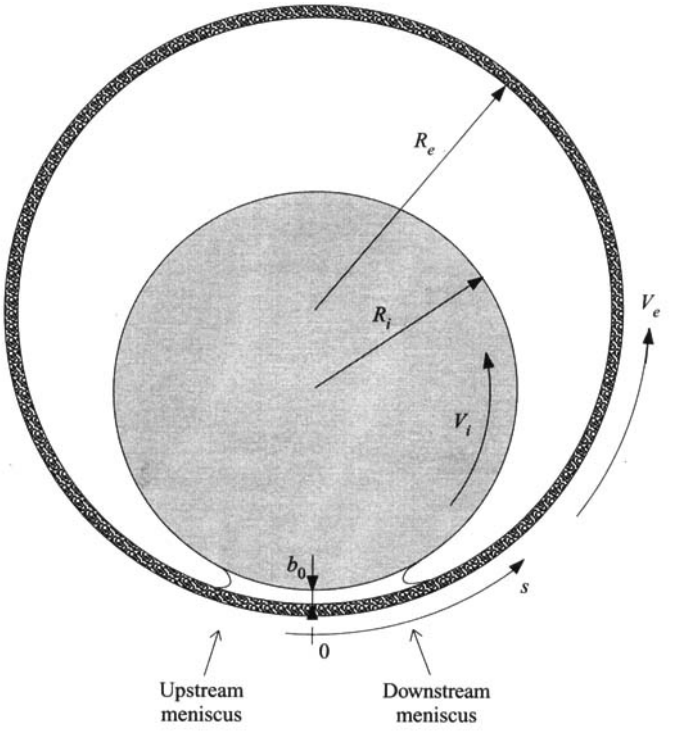

FIGURE 1. Cross-section of the experimental set-up. The radii of the cylinders are $R_i = 33 \pm 0.02$ mm and $R_e = 50 \pm 0.05$ mm, their lengths are 380 and 420 mm respectively. The minimum gap b_0 is 0.30 ± 0.05 mm. The curvilinear abscissa, s, lies on the outer surface of the outer cylinder. It is oriented downstream (here to the right) and its origin is located at the position of minimum thickness. The upstream meniscus is on the left and the downstream meniscus on the right.

& Couder 1990; Michalland, Rabaud & Couder 1993; Cummins, Fourtune & Rabaud 1993, Pan & de Bruyn 1993; Decré 1994) which affects the meniscus of a viscous fluid placed between non-parallel moving walls.

This latter instability occurs in several industrial coating processes (where it is usually called the ribbing instability) as well as in journal bearings (Taylor 1963). In previous work we have introduced a system where this instability occurs in a narrow gap between two cylinders placed one inside the other (Rabaud *et al.* 1990; Michalland 1992) and rotating with two independently tuned velocities. Directional viscous fingering then affects the meniscus situated on the widening side with respect to the direction of the mean velocity of the two cylinders. Like Saffman–Taylor fingering (Saffman & Taylor 1958), the instability is due to the displacement of a high-viscosity fluid (oil) by a low-viscosity fluid (air). Both the surface tension and the thickness gradient between the cylinders act as stabilizing factors. This instability, which was also called the printer's instability, was shown (Rabaud *et al.* 1990; Cummins *et al.* 1993) to have a rich variety of dynamical regimes because the velocities of the two walls form two independent control parameters. A recent theoretical work by Reinelt (1995) gives an analysis of the position of the menisci and of their stability.

The present work describes instabilities which occur in the same experimental set-up but which affect the front situated on the narrowing side of the gap, a front which was until recently thought to be stable. Preliminary results about this instability were presented by Michalland (1992). In the following, after a description of the set-up (§2), we will present successively the two different transitions which are observed (§3). In the

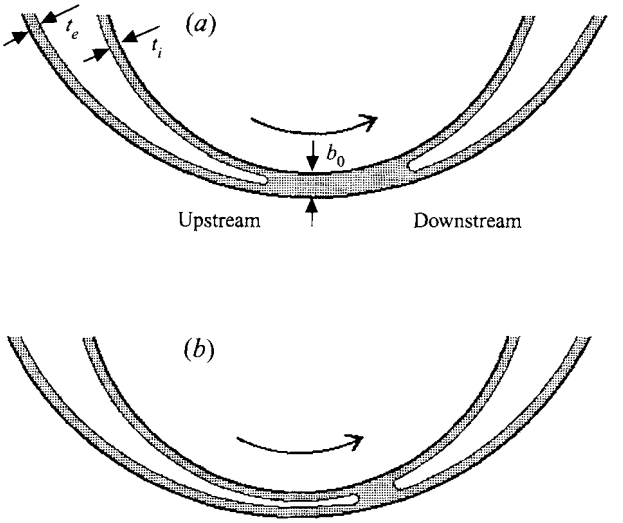

FIGURE 2. Sketch of the positions of the menisci in a cross-section of the set-up: (*a*) upstream meniscus at $s_u < 0$, (*b*) upstream meniscus at $s_u > 0$. t_i and t_e are respectively the thickness of the oil films on the inner and outer cylinder.

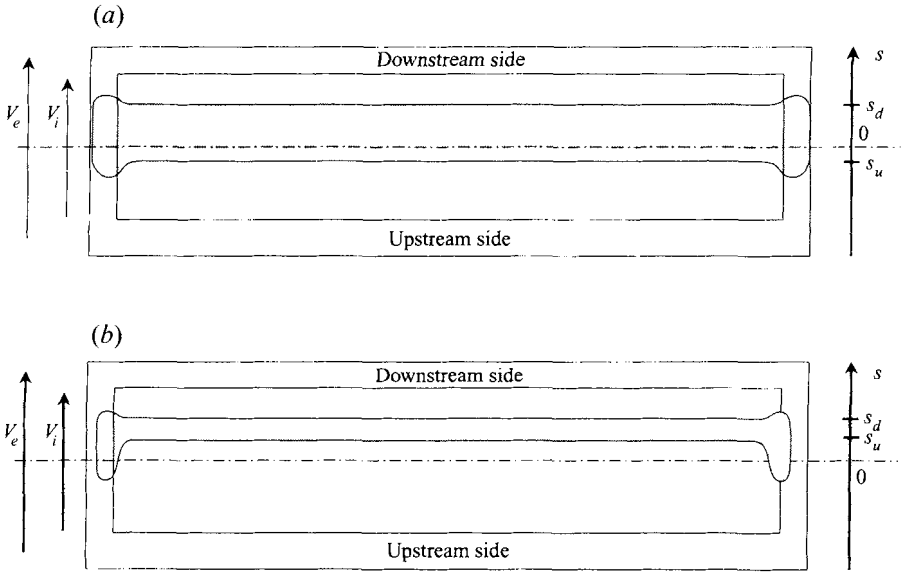

FIGURE 3. Sketch of the position of the two menisci seen from below at small velocities. As in all the other figures the velocities are directed from the bottom to the top. The position of the minimum thickness is given by the broken line. The abscissa s is oriented towards the top of the figure, in the direction of V_i and V_e. The region of the gap completely filled by oil is shown in grey. (*a*) Filling of type B; (*b*) filling of type C, with a smaller initial oil volume.

first one the linear front undergoes a supercritical transition to standing or propagating waves (§3.3). In the second, finite-amplitude fingers are formed after a subcritical bifurcation (§3.4). These fingers present several secondary bifurcations leading to specific dynamical behaviour (§3.6). The results are discussed in §4.

2. Experimental set-up

The experimental set-up is identical to that used in Rabaud *et al.* (1990) to study the printer's instability. A sketch of a transverse section of the cell is given in figure 1. It is formed of two horizontal glass cylinders, of radii $R_i = 33 \pm 0.02$ mm and $R_e = 50 \pm 0.05$ mm and lengths 380 mm and 420 mm respectively. They are placed one inside the other, off-centred so that, at the bottom of the apparatus, their surfaces are separated only by a small gap along a generatrix (figure 1). The minimum spacing b_0 between them can be adjusted. In the present experiments $b_0 = 0.3 \pm 0.05$ mm is chosen. A small amount of a viscous liquid is introduced between the cylinders at the beginning of the experiment so that it only fills the lower part of the gap. The fluid we used was a silicone oil (Rhodorsil 47V100) with a viscosity $\mu = 96.5\ 10^{-3}$ kg m^{-1} s^{-1} and a surface tension $T = 20.9\ 10^{-3}$ N m^{-1} at 25 °C. This oil wets the glass surfaces of the cylinders perfectly. As we will see our results depend on the quantity of oil placed in the cell. The two cylinders can be set in rotation independently by two regulated DC motors. We will call the tangential velocity at the periphery of the inner cylinder V_i and the velocity of the inner wall of the external cylinder V_e. These velocities can be tuned typically from 0 to 100 mm s^{-1}. The lower region of the apparatus is observed from below by a CCD video camera. Two lines are observed which correspond to the two menisci limiting the domain where the gap is completely filled by oil. The menisci positions are characterized by their curvilinear abscissa s along the periphery of the external cylinder. The origin is taken at the point of minimum thickness and s is chosen positive in the direction of the mean flow $(V_i + V_e)/2$. Positive values of s thus correspond to the downstream side, and the negative ones to the upstream side (figure 1). The menisci seen from below are straight when stable but become periodically distorted when unstable. In order to characterize the instabilities of a meniscus the video pictures were digitized and analysed on a Macintosh II× computer using the freeware Image 1.4. A particularly useful type of image processing was aimed at the direct observation of the spatio-temporal evolution of the front. One single video-line parallel to the front was chosen so that it intercepts all the cells of the pattern. At fixed time intervals we recorded this line and then, by collecting successive lines, we reconstructed a new image showing the time evolution of the pattern.

All the previous experiments on the ribbing instability were concerned with the behaviour of the meniscus in the region where the two solid surfaces move away from each other. In the following we will call this front the downstream meniscus. In the present set-up this downstream front is unstable by the usual printer's instability when V_i or V_e (or their average) become larger than typically 50 mm s^{-1}. In contrast, the new instability occurs on the upstream meniscus for much smaller velocities, of the order of 10 to 25 mm s^{-1}. This instability had probably remained unnoticed because it is only observed if some care is taken concerning the total quantity of liquid present in the system.

3. Experimental results

3.1. *Position of the menisci*

When the whole apparatus is at rest, all the oil is at the bottom of the cell and the two menisci are at the same horizontal level. Except near the extremities the menisci form two straight lines symmetrical with respect to the line of minimum thickness at a distance $\pm s_0$ from it. As the cylinders are rotated, a wetting film forms on their surfaces and the quantity of oil left at the bottom is decreased. Therefore the first effect of the rotation is to shift the position of the two menisci towards the bottom of the cell. The films thickness could be in principle deduced from the position of the menisci if the flow was strictly two-dimensional. But in reality the lateral boundaries of the front have to be taken into account. In our system the outer cylinder is longer than the inner one. As a result, when the quantity of oil introduced in the cell is large, the excess oil is observed to accumulate in this region. Three types of situations (labelled A, B or C) are observed, depending on the amount of oil introduced in the cell initially.

Case A: If there is a large quantity of oil the position of the upstream meniscus does not change much when the system is set into rotation. At large velocities the downstream meniscus recedes so that its abscissa s_d decreases. Correspondingly, the upstream region forms a reservoir for the excess oil. In this situation the printer's instability modes are easily observed on the downstream front; they are only weakly dependent on the total amount of oil. The upstream meniscus is then always stable, and none of the effects that we are going to describe takes place.

Case B: If there is a smaller quantity of oil, the observed processes are quite different. When the cylinders start rotating with a small mean velocity $(V_i+V_e)/2$, the upstream front starts moving downstream and settles at a well-defined position s_u (figure 2). This distance from the minimum gap depends on V_i and V_e. The upstream meniscus takes up its preferential positions s_u along most of the cylinders' length. The excess oil moves to the extremities of the cylinder where it collects in a recirculation zone. Figure 3(*a*) is a sketch of the positions and shapes of the two menisci as seen from below. Only the linear part of the front at s_u will undergo the sequence of bifurcations to be described below.

Case C: When the quantity of oil introduced in the cell is even smaller, the amount left at the bottom after coating the cylinders is small. In this case the upstream front will not be able to stabilize in the previous position. It drifts past to the other side of the line of minimum thickness and settles at a new stable position (figures 2*b* and 3*b*): s_u is then positive. The oil at the bottom is then entirely on the downstream side of the minimum gap.

Figure 4(*a*) shows (for cell filling of type B) the evolution of the positions of the upstream and downstream menisci s_u and s_d as a function of the velocity V_e of the outer cylinder for a fixed value of velocity of the inner cylinder V_i. The upstream meniscus is stable at low velocity, then undergoes two successive bifurcations where the front becomes unstable so that s_u has two values corresponding to the extrema of the front's position. The instability of the downstream meniscus occurs at a larger velocity, outside the range shown here.

Similar plots of the position of the two menisci for cell filling of type C are shown on figure 4(*b*), as a function of V_e for three fixed values of velocity of the inner cylinder V_i. For the largest velocity V_i the upstream meniscus is advected to positive values of s before becoming unstable to a finite-amplitude disturbance. In the following our investigation will concentrate on a situation where the filling is of type B, but consideration of case C will also be useful.

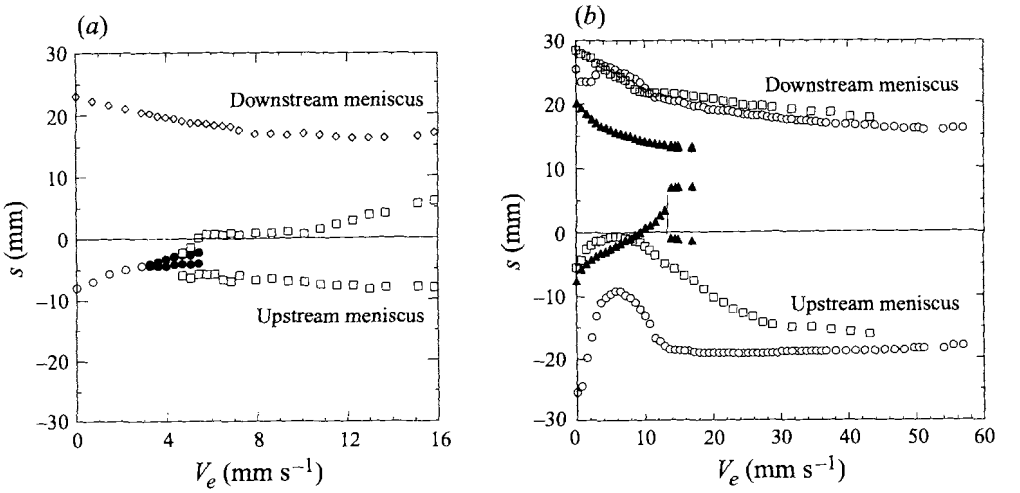

FIGURE 4. Position of the two menisci s_d and s_u as a function of the increasing velocity of the outer cylinder V_e for fixed values of V_i and for two types of filling of the cell. (*a*) Filling B for $V_i = 12$ mm s^{-1}, chosen in the range where the upstream menisus can become unstable: ◇, stable downstream meniscus; ○, stable upstream meniscus; ●, extrema position of the upstream interface in the standing wave regime; ⊡, positions of the extrema of the upstream interface when fingers are observed. Note that there is a hysteretic domain ($4.5 < V_e < 5.5$ mm s^{-1}) in which oscillations are observed for increasing V_e and fingers for decreasing V_e. (*b*) Filling C for three values of V_i: ⊙, $V_i = 0$; □, $V_i = 5.6$ mm s^{-1}; ▲, $V_i = 8.7$ mm s^{-1}. For the first two values the upstream front is stable. For the third the front recedes and passes to an $s_u > 0$ position before undergoing a subcritical bifurcation where there is formation of oil fingers with their tip located at $s < 0$. Note that when $V_i \neq 0$, s_d and s_u are not equal at $V_e = 0$ because of the rotation of the inner cylinder.

3.2. *The domains of instability of the two menisci*

The precise investigation of the different instabilities of the upstream front is much more difficult than that of the printer's instability for three reasons.

(i) The main problem is the direct coupling of the two menisci. Because the system is closed, the oil which reaches the upstream front is what is contained in the two films which have left the downstream front. A change of the velocities of the cylinders induces a change in the thickness of the deposited films. However, this change will only be observed on the upstream front after a full period of rotation of the slower cylinder.

(ii) A related difficulty is that any local disturbance of the downstream front will influence the upstream one (the reverse is not true, hence the robustness of the printer's instability). In particular the presence of a bubble on the downstream front will induce a local decrease of the thickness of the film generated in this region and a strong disturbance of the upstream front in this region.

(iii) The third difficulty is linked with the subcritical character of one of the observed transitions. In the hysteresis region we have observed the coexistence of different domains, to be described below, which could be very sensitive to imperfections of the system. Indeed defects in the gap value (both in eccentricity and spanwise spacing) result in spatial and temporal fluctuations in the direction and value of the thickness gradient vector. The effect of these irregularities, however, is only important when the menisci are close to the gap and when the velocities are in the immediate vicinity of the various thresholds.

Figure 5(*a*) shows a general sketch of the stability diagram for both menisci (with filling of type B) as a function of the rotation velocities V_i and V_e of the two cylinders. For the stability of the downstream meniscus we recover the results obtained

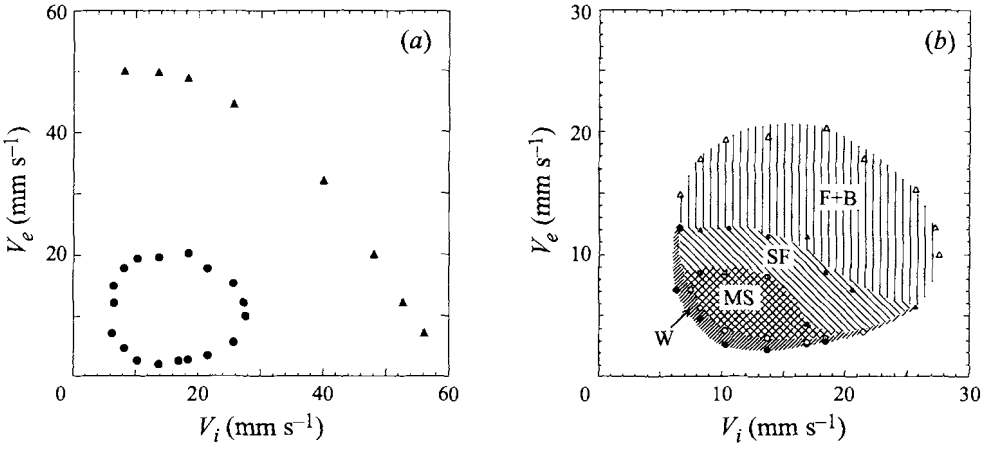

FIGURE 5. (*a*) Stability diagram of the upstream meniscus and downstream meniscus in the plane of the cylinder velocities V_i and V_e. The triangles (▲) represent the onset above which the downstream meniscus is unstable. The upstream meniscus is only unstable inside the closed area limited by the black dots (●). (*b*) Close-up of the region on the phase diagram in which the upstream meniscus is unstable, divided into four sectors. In zone W, one can observe standing waves or travelling waves. In zone MS, there is coexistence of several states: waves, solitary fingers, travelling fingers and steady fingers. In zone SF the front forms a well-defined pattern of steady fingers. Finally, in the region F + B the fingers are unstable and emit bubbles.

previously in the investigation of the printer's instability. The upstream meniscus is only unstable for co-rotating cylinders (V_i and $V_e > 0$) and close to the first diagonal ($V_i \approx V_e$). It was found to always be stable when either one cylinder was at rest or when the cylinders were counter-rotating. Furthermore, the instabilities were only observed in a finite range of values of V_i and V_e so that they were limited to a closed domain of the diagram (figure 5*a*, *b*). This domain corresponds to velocities smaller than those of the printer's instability so that the two menisci are never unstable simultaneously.

To a first approximation the state of the new instability depends mainly on the mean rotation $(V_i + V_e)/2$. However, as shown on figure 5(*b*) the onsets are not completely symmetrical with respect to the first diagonal in the diagram (V_i, V_e). Note that in this respect our system is not symmetrical for two reasons. The first is the possible role of gravity on the flow; the second is the geometry of the cell ($R_e > R_i$). For instance, when the velocities are exchanged the amount of oil used to coat the cylinders will not be the same because of the difference in size of the cylinders. As a result the quantity of oil left at the bottom will not be the same.

Two main types of instabilities are observed to affect the upstream meniscus, having respectively small and large amplitudes. We performed a systematic investigation of their domains of existence in the case of cell filling of type B. In practice most of the instability diagram was explored by increasing V_e while the velocity of the inner cylinder V_i was kept constant. Figure 4(*a*) shows the position of the two menisci with respect to the minimum gap during such an increase of V_e (for $V_e = 12$ mm s^{-1}). A complete investigation was not done in the case of type C filling because in this case the threshold values depended on the precise filling of the cell. We will however discuss qualitatively the effects observed for filling of type C as they turn out to be very revealing about the nature of the instability.

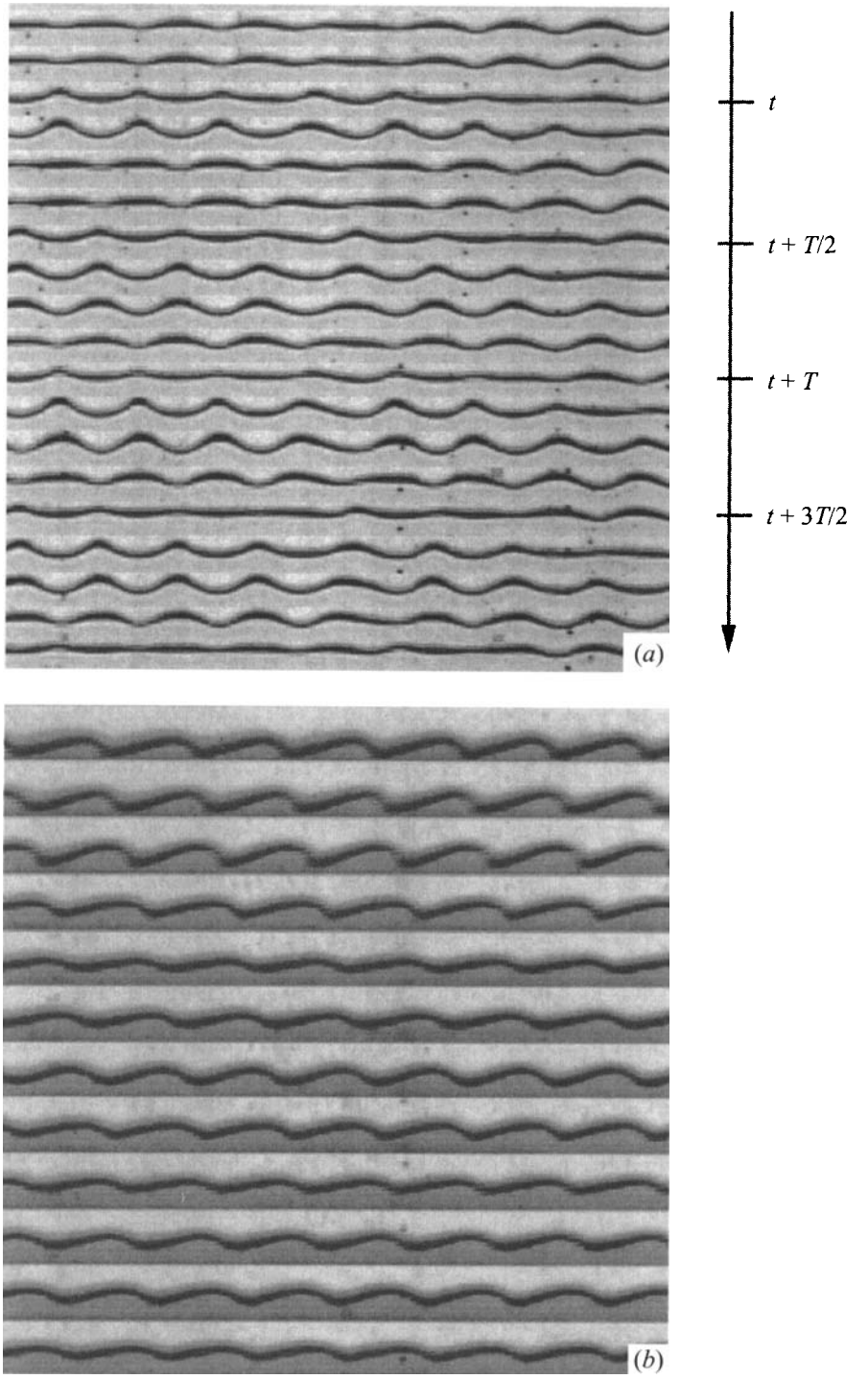

FIGURE 6. (*a*) Successive photographs of a standing wave observed for $V_i = 10.8$ mm s^{-1} and $V_e = 2.9$ mm s^{-1}. As in all photographs of the front, the region occupied by oil is above each interface and the region occupied by air below. The wavelength is $\lambda = 5.7$ mm and the maximum amplitude is of the order of 1 mm. The time periodicity is $T \approx 0.7$ s and the corresponding phase velocity is $U = \lambda/T \approx 8.1$ mm s^{-1}. The period T is small compared to the period of rotation of both cylinders (respectively 17 and 108 s). (*b*) Successive photographs of a propagating wave (to the right) observed for $V_i = 13.6$ mm s^{-1} and $V_e = 2.9$ mm s^{-1}.

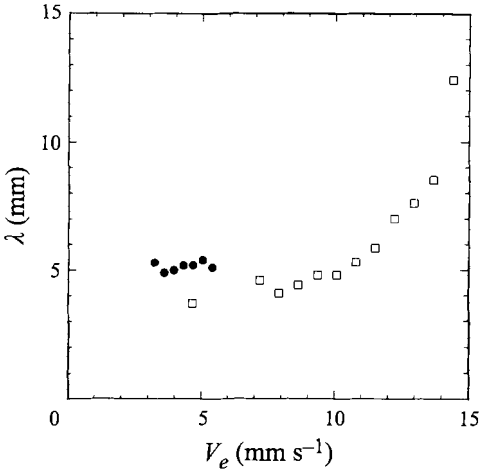

FIGURE 7. Evolution of the pattern wavelength λ as a function of V_e at a fixed value $V_i = 12$ mm s^{-1}. The black dots (●) show the wavelength of the waves, the squares (⊡) the wavelength of the fingers. There is a strong increase of this wavelength with increasing V_e which seems to correspond to a divergence when V_e reaches 15 mm s^{-1}. This leads to the restabilization of the front. The values close to the divergence were averaged because at this point the pattern is no longer periodic. No measurements could be made very near the limit value.

3.3. *The instability to standing or propagating waves*

3.3.1. *Filling of type B*

Let us now describe the instabilities as they are observed in a case such as that depicted on figure 4(*a*). The inner cylinder rotates at a fixed velocity $V_i = 12$ mm s^{-1}. With the increase of V_e the upstream meniscus first recedes towards the minimum gap, remaining straight. Above a critical value $V_e = 3.1$ mm s^{-1}, which is the threshold of the first instability, the upstream meniscus becomes wavy with a sinusoidal shape. This instability is always time dependent: the pattern either oscillates as a standing wave (figure 6*a*) or moves as a propagating wave in either of the two possible directions (figure 6*b*). Just above the onset of the transition (for $V_e = 3.1$ mm s^{-1} and $V_i = 12$ mm s^{-1} the measurements show a continuous increase of the amplitude of the sinusoid with the distance to the onset (as can be seen on figure 4*a*). On the other hand the frequency of the oscillations is finite at the threshold and approximately constant in its vicinity. Therefore the transition has the characteristics of a supercritical Hopf bifurcation. Measurements of the wavelength of the pattern show it to be well defined: for instance it is $\lambda_c = 5.7$ mm in the case shown on figure 6(*a*). At these values the period of the oscillations of the standing waves is typically 0.7 s so that the corresponding propagation velocity is 8.1 mm s^{-1}. Figure 7 is a plot of the wavelength of these patterns as a function of the imposed V_e, showing that in their narrow range of existence the wavelength of these waves is constant. The domain of existence for these waves (standing or propagating) is shown on the stability diagram for the upstream meniscus on figure 5(*b*), obtained as a function of V_i and V_e with filling of type B.

A discussion of the dynamics of travelling and standing waves in nonlinear systems can be found in Cross & Hohenberg (1993). A usual situation of nonlinear dynamics (e.g. the travelling modes of the printer's instability, Cummins *et al.* 1993) is that travelling waves moving in one direction have an inhibiting influence on the travelling waves moving in the opposite direction so that standing waves are not observed. In

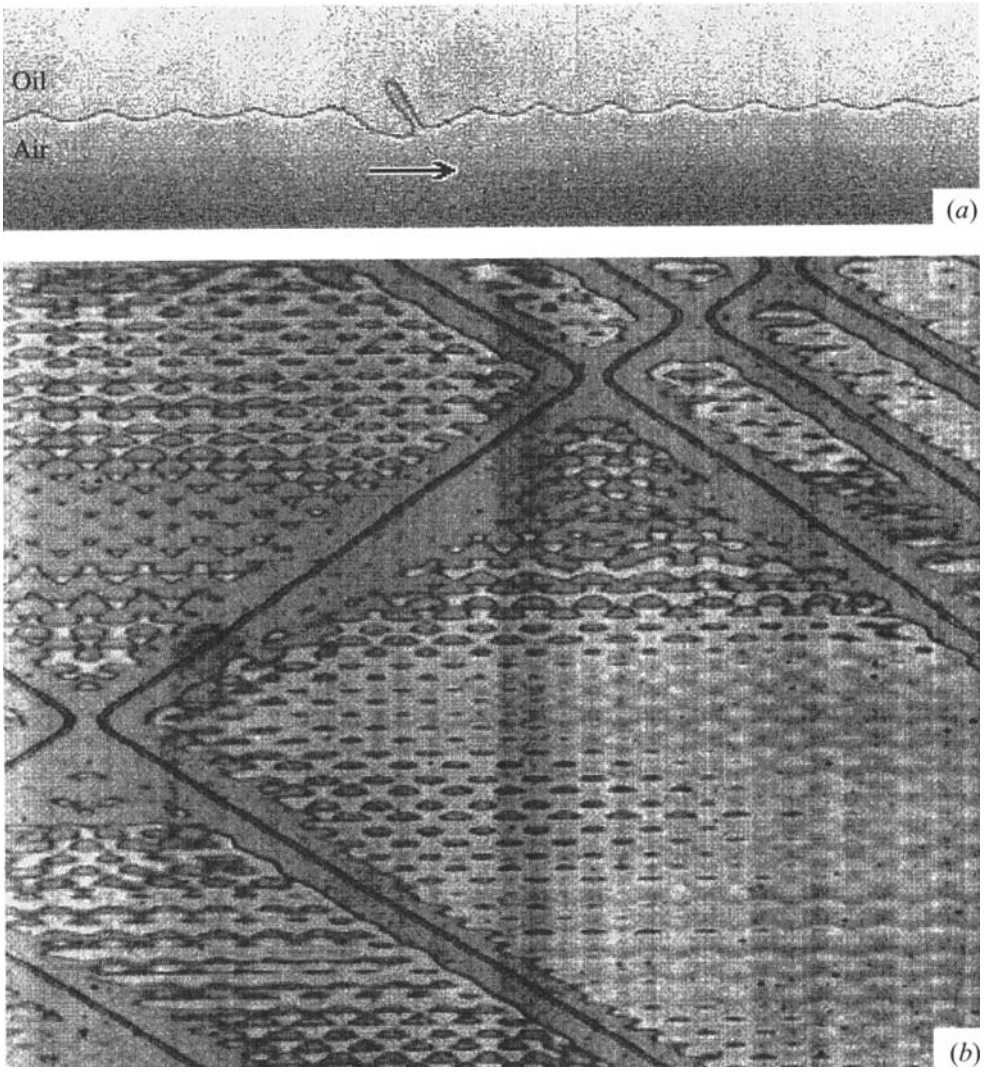

FIGURE 8. The fingers often appear initially as solitary structures which travel back and forth along the front. Here $V_i = 12.2$ mm s^{-1} and $V_e = 3.3$ mm s^{-1}. (*a*) The front with a solitary finger running on a front with standing waves. (*b*) Corresponding spatio-temporal behaviour. Time increases from the top of the figure to the bottom by 25 s. Several solitary waves are observed travelling and undergoing elastic collisions.

other situations, however, the existence of the two types of waves is possible. This is the case for instance in the Faraday experiments (Douady, Fauve & Thual 1989). The two types of waves are then observed for different values of the control parameters and a change of these parameters generates a continuous transition from one mode to the other.

In the present experiment however the two types of waves appear to coexist in the same range of values of the control parameter. It is possible that the criterion of selection of these two waves remained unresolved because their domains of existence were too narrow for the precision of our experiment.

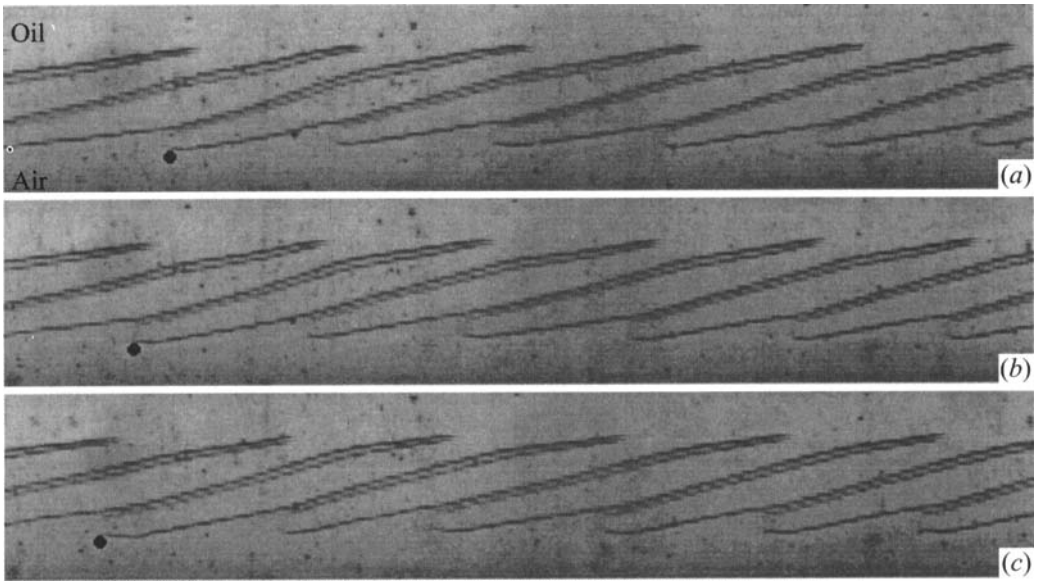

FIGURE 9. Time sequence of an array of propagating fingers observed for $V_i = 11.6$ mm s^{-1} and $V_e = 5.1$ mm s^{-1}. The wavelength of the pattern is of the order of 13 mm. Here, the fingers propagate to the left (as shown by the black dot) with a velocity of 33 mm s^{-1}.

3.3.2. *Filling of type C*

For this filling and at the velocities for which the wave instability should exist the upstream meniscus is on the downstream side of the gap ($s_u > 0$). The wave instabilities were never observed in such situations.

3.4. *Fingering instability*

3.4.1. *Onset of the finger formation: type B filling*

Above a second threshold (at $V_e = 5.5$ mm s^{-1} on figure 4*a*) we enter a domain labelled MS in the phase diagram of figure 5(*b*). This region is complex as it is characterized by the competition between several types of instabilities. On passing the threshold the first effect is the appearance of localized disturbances consisting of two protrusions separated by a deep and narrow air tube penetrating the front and reaching the region of minimum thickness (figure 8*a*). The air tube is tilted and the whole structure travels fast along the wavy front. The amplitude of these propagating fingers is large in comparison with that of the wavy instability. They are at first solitary structures and mostly form near the two extremities of the front. When two of these structures travelling in opposite directions meet, they usually have an apparently elastic collision (figure 8*b*). Similar structures have been observed in front instabilities by Rabaud *et al.* (1990) in the printer's instability (in a contra-rotating situation) and by Melo & Douady (1993) on the front of a viscous fluid flowing down inside a rotating cylinder.

For slightly larger velocities these travelling structures form in packets and invade the whole front, forming a complete array of propagating fingers (figure 9). Their velocity is large: for instance on figure 9 where $V_i = 11.6$ mm s^{-1} and $V_e = 5.1$ mm s^{-1} they propagate at 33 mm s^{-1}. Because the two directions of propagation (right and left) are equally probable the pattern can have some sources (singular points from which the moving fingers emerge) and sinks (singular points of the front where the fingers coming from opposite directions vanish).

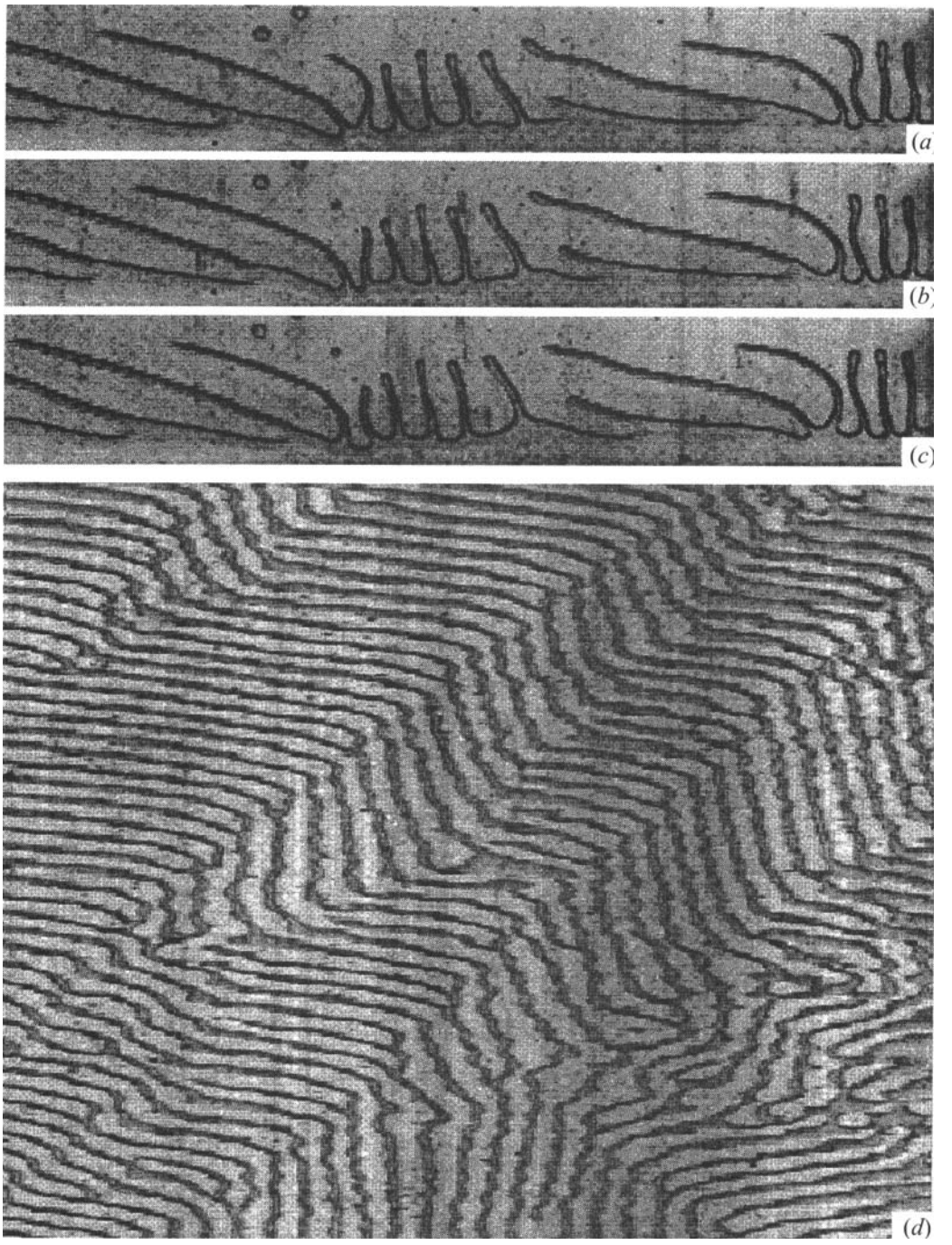

FIGURE 10. The coexistence of steady and travelling fingers observed at $V_i = 13\ \text{mm s}^{-1}$ and $V_e = 6.4\ \text{mm s}^{-1}$: (*a*, *b*, *c*) three successive photographs of the front, (*d*) corresponding spatio-temporal evolution of the front for a period of about 10 s.

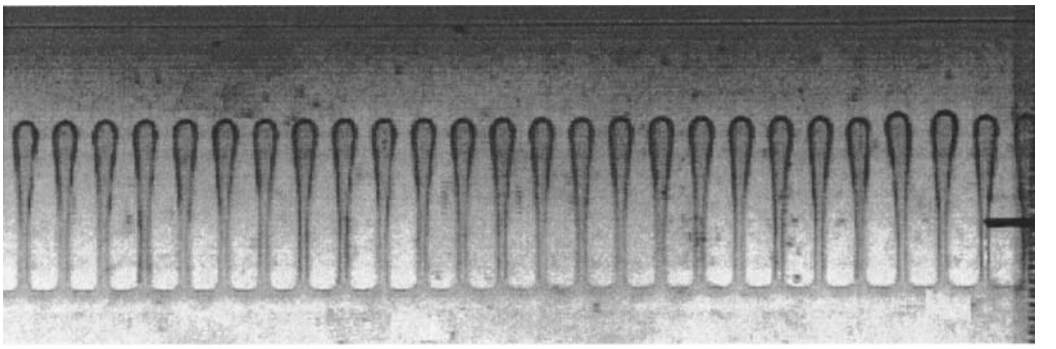

FIGURE 11. An array of steady fingers observed for $V_i = 8.9$ mm s^{-1} and $V_e = 10$ mm s^{-1}. The wavelength of the pattern is of the order of 4 mm. The black tick on the right of the picture shows the position of the minimum thickness at $s = 0$. The stable downstream meniscus is visible at the top of the picture.

For still larger velocities regions of the front appear where the travelling fingers stop and become steady. Figure 10 shows the front in this regime of coexistence of domains of travelling and steady fingers. Figure 10(*d*) shows the corresponding spatio-temporal behaviour.

Finally the region labelled SF on figure 5(*b*) is reached. In this domain a regular pattern of steady fingers is observed. The shape of these fingers can be seen on figure 11. It is a sort of reverse of the air fingers usually observed in directional viscous fingering. Here the fingers are formed of oil and their tips, which are rather flat, are always located on the upstream side of the gap. These fingers are separated from each other by tubes filled with air which penetrates beneath the inner cylinder. An important characteristic is that the extremity of these tubes usually reaches the downstream side of the gap (see figures 4*a* and 11). The shape of these air tubes is dominated by surface tension so that their local width varies with the local thickness. As a result, their width is minimum and of the order of b_0 at $s = 0$ as shown on the photograph of figure 11.

The existence of the domain MS can now be interpreted in the following way. The formation of the fingers (whether travelling or steady) is a finite-amplitude disturbance of the front. Although the two states (waves and fingers) are very different in shape and amplitude, the limit in the phase diagram between them is not easy to define. The limit between region W and MS fingers drawn on figure 5(*b*) corresponds to the lowest value for which fingers are observed. The transition however exhibits a strong hysteresis and is therefore a subcritical bifurcation. For increasing velocities, the transition is preceded by a regime of travelling fingers with, as noted above, coexistence of spatial domains which are in different regimes. In reverse, for decreasing velocities, no travelling fingers or solitary waves are observed.

3.4.2. *Onset of the finger formation: type C filling*

If the quantity of oil in the cell is small, in the presence of rotation the upstream meniscus drifts until it is located at positive values of s (on the downstream side of the gap (figures 2*b* and 3*b*). In this situation the first instability to waves is not observed and a direct transition to a pattern formed of fingers will be observed at larger velocities. It is a very subcritical event in which the mean position of meniscus jumps from one side of the minimum gap to the other (*i.e.* from positive to negative s). At this transition there is a range of values where there can be coexistence of the two states.

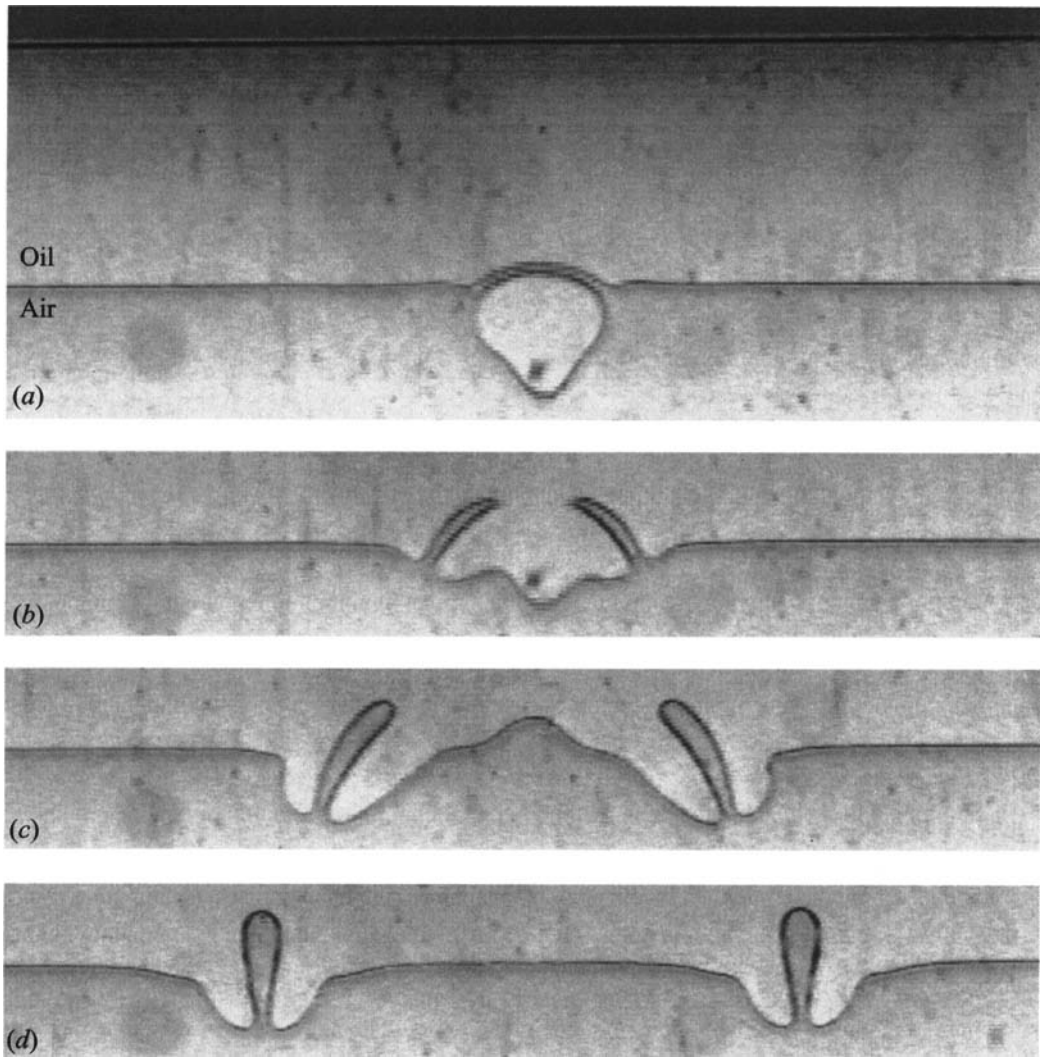

FIGURE 12. Four successive video images showing the effect of an impinging region of thicker coating film on a stable upstream meniscus located at $s_u > 0$ (filling is of type C). The final state (d) is formed of two localized structures in which the meniscus has moved to $s < 0$ on each side of a penetrating air tube.

This is illustrated by the sequence of images of figure 12 showing a typical event that occurs just below the spontaneous transition to fingers when a finite size disturbance reaches the front. In this particular instance a speck of dust was present in the cell. Upon leaving the downstream meniscus an excess of oil had accumulated around it. After rotation of the outer cylinder, this zone collided with the upstream meniscus. Locally the film was too thick to pass the minimum gap without touching the inner cylinder so that in this region the meniscus jumped ahead of the minimum gap (figure 12a). Simultaneously the air film that separated the 'drop' from the front broke and survived as two narrow penetrating air tubes. Two local disturbances similar to the solitary waves shown on figure 8(a) were thus generated, propagating respectively to the left and the right (figures 12b, c). The difference with the previous case is that they

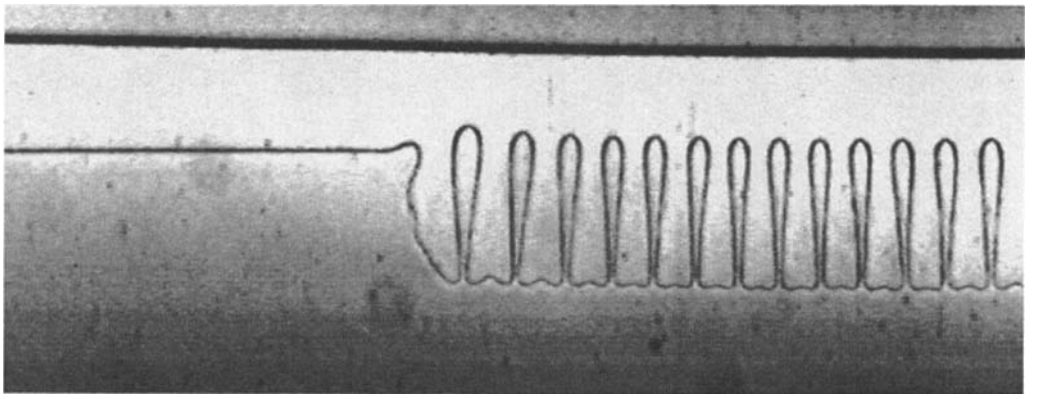

FIGURE 13. The subcritical transition observed in filling of type C, from a stable linear front located at $s_u > 0$ to a front formed of parallel fingers with their tips located at $s_u < 0$. As the velocities are above the threshold of formation of the fingers, the left side of the finger domain moves to the left as new fingers are formed. Finally the whole front is invaded by the fingers.

spontaneously stopped at a certain distance from each other and then remained stable and steady (figure 12*d*).

Let us now return to an undisturbed situation. With the increase of the velocities the two coating films leaving the downstream front become thicker. As a result they become unable to pass through the minimum gap without touching each other. They do so at various nucleation sites along the front. In these regions a front with steady fingers sets in directly. The fingers are identical to those described above with their tips upstream and the extremity of the air tubes downstream. The domains will expand and ultimately invade the whole front. The front during the transient is shown on figure 13.

3.5. *The restabilization of the front*

The domain of existence for the fingering instability shown on figure 5 is limited. With increasing velocities the upstream front restabilizes. There are two precursors to this restabilization: the pattern's wavelength tends to increase as shown on figure 7 and the fingers start emitting bubbles. The domain in which this formation of bubbles occurs is labelled F + B on figure 5(*b*).

3.5.1. *Formation of bubbles*

With the increase of the velocity two effects are observed. First the air tubes become longer, their downstream extremity becoming inflated into an attached bubble (figure 14*a*). Simultaneously the tube by which each bubble remains attached to the front becomes thinner and thinner in the minimum gap region. Ultimately the tube will break when the drag is large enough to overcome surface tension. Detached bubbles are thus formed (figures 14*b*, *c*) and advected to the downstream front by the mean flow of oil. This behaviour is reminiscent of the regime of formation of bubbles observed in directional growth of liquid crystals (Flesselles *et al.* 1991) and in directional solidification of plastic crystals (Kurowski *et al.* 1989; Brattkus 1989).

3.5.2. *Restabilization of the front*

At larger velocities the frequency of detachment of these bubbles increases. At this point the situation becomes confused because more and more bubbles form and accumulate on the downstream front. On the upstream front, with the trend for a

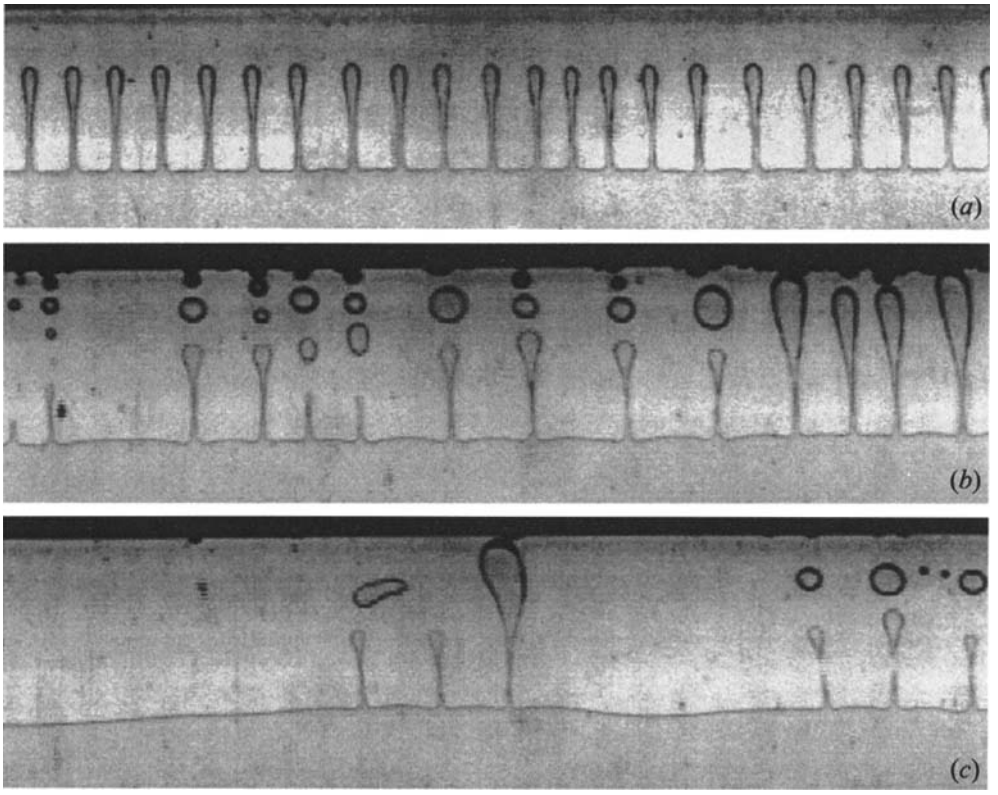

FIGURE 14. Photographs obtained for increasing values of V_e showing the evolution leading to the formation of bubbles. V_i was constant at 11.4 mm s^{-1}. (*a*) V_e = 12.1 mm s^{-1}, (*b*) V_e = 16.4 mm s^{-1} and (*c*) V_e = 17.1 mm s^{-1}.

narrowing of the air tubes separating the fingers, they become so narrow that they vanish. The mean wavelength of the pattern thus increases with the increasing velocities (figure 7). At large velocities this wavelength becomes very uneven: only an average value is shown on figure 7. Correspondingly, as the wavelength tends to diverge, the upstream front returns to a stable state (figure 14*c*). We thus move out of the instability area and both menisci become flat and stable again. Because of the disturbing influence of the bubbles, this limit is generally ill-defined. In order to measure it we adopted the following procedure: we first increase the velocities of the motors in such a way as to get around the unstable region and reach values of V_i and V_e situated above it. The front is then stable and by reducing V_e we obtain the upper limit of the instability with a much better accuracy (it is the limit which is drawn on figure 5*b*). This restabilization of the front at large velocity is reminiscent of a similar behaviour observed in the directional growth of liquid crystals (Simon & Libchaber 1990). However, in that case the wavelength vanished at the restabilization threshold, whereas here it diverges (figure 7).

3.6. *Secondary instabilities of the fingers*

In the region SF where the front is generally formed by steady periodic fingers two secondary instabilities were occasionally observed. However, their region of existence was not determined as their formation appeared to depend on the filling and on the way in which the velocities had been increased.

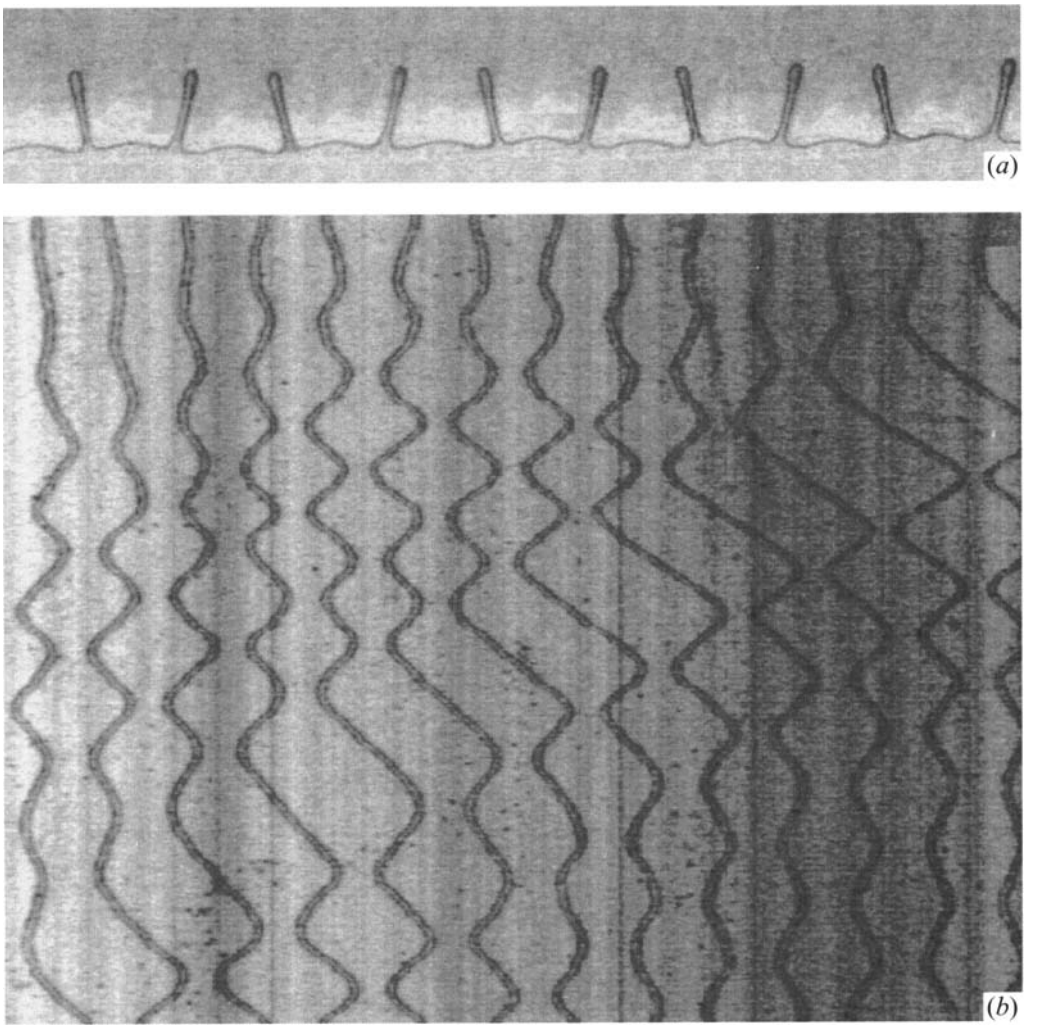

FIGURE 15. The oscillations of the air tubes in an out-of-phase mode observed at $V_i = 12.1$ mm s^{-1} and $V_e = 3.2$ mm s^{-1}. The period is of the order of 1 s. (*a*) The front and (*b*) the corresponding spatio-temporal evolution. A wave propagating from right to left is also visible on (*b*).

3.6.1. *Oscillation of the tube positions*

In the first mode, which is observed just above the region of existence of the solitary waves, the air tubes oscillate so that the fingers separating them have an oscillating width. In this regime neighbouring fingers oscillate in opposite phases as seen on figure 15. Each air tube can be considered as undergoing periodic collisions with its neighbours, these collisions being of the same type as those shown on figure 8(*b*). Indeed there is an almost continuous transition between the solitary wave regime and the oscillation.

3.6.2. *Oscillation of the front of the fingers*

In a limited region of the phase diagram, a second type of instability also appears in which there is a self-sustained oscillation of the tips of the fingers. Successive states of this oscillation are shown on figure 16. It forms a superimposed standing wave with a wavelength equal to twice that of the fingers. The temporal oscillation of the structure

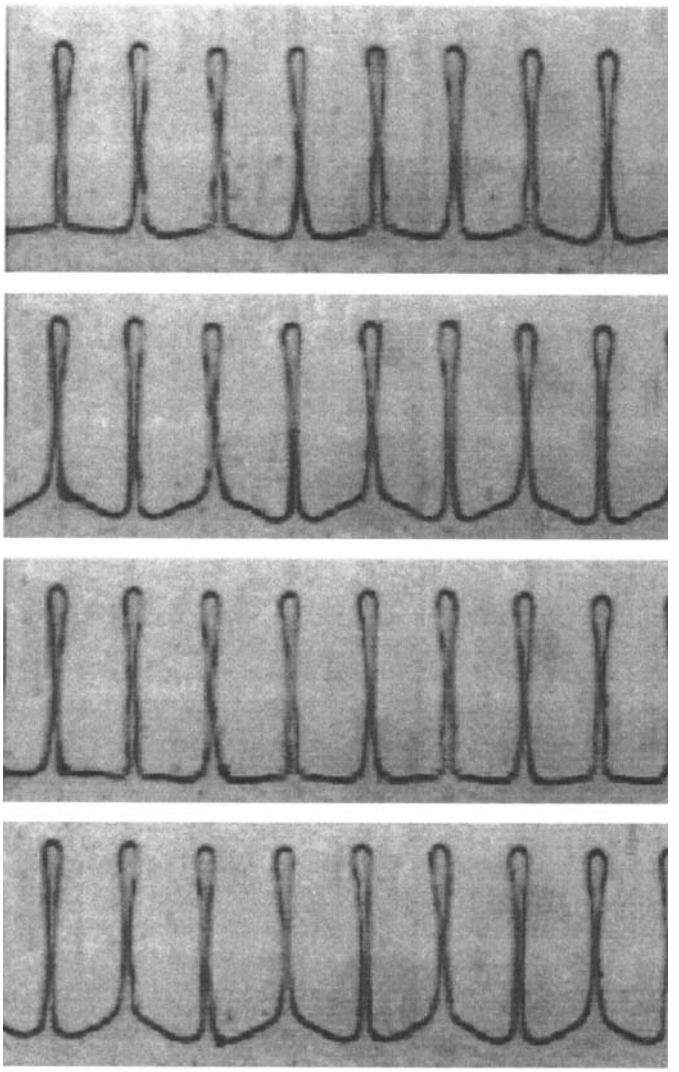

FIGURE 16. Four successive photographs of the fingers in their oscillation regime at the instants $t \approx 0$, $T/4$, $T/2$ and $3T/4$; $V_i = 11.4$ mm s^{-1} and $V_e = 8.2$ mm s^{-1}. The finger wavelength is $\lambda = 5$ mm and the wavelength of their modulation is twice as large. The period T of the oscillation is approximately 2 s.

occurs with a typical periodicity of 2 s in the case of figure 16. This time-dependent mode is one of the ten destabilization modes of a one-dimensional pattern described by Coullet & Iooss (1990), a mode that has been only recently experimentally observed (Valette, Edwards & Gollub 1994).

4. Discussion

In very general terms the observed instabilities affect the front formed when two films coating two solid surfaces meet in a narrowing, then expanding gap. In the present situation the analysis of this instability is complex because it involves a coupling between the two menisci present in the cell: the corotation of the cylinders brings back upstream the films formed downstream.

4.1. *Position of the menisci*

4.1.1. *Conservation of the oil and the two-dimensional hypothesis*

At the beginning of the experiment a given quantity of oil is introduced in the cell and lies at the bottom of the cell. When the two cylinders are set into rotation they extract two oil films which cover their surfaces so that the quantity of oil left at the bottom is reduced and the two menisci recede towards $s = 0$ as shown by figure 4. In principle the quantity of oil in a given section of the cell should be constant, the part of it spread in the films being a function of the velocity. The existing analyses (Hakim *et al.* 1990; Reinelt 1995) rely on this two-dimensional hypothesis in which all the flow in all transverse sections of the cells is identical. In reality this is an approximation: as already observed in the investigation of the printer's instability (Rabaud, Couder & Michalland 1991) when a large amount of oil is introduced in the cell, the excess oil is progressively rejected to the extremities of the cylinders where it accumulates (figure 3*a*). Thus in general the quantity of fluid present in one section of the set-up is not necessarily constant. A direct measurement of the film's thickness would be necessary to check this point. It was not feasible in our device so that we were not able to quantify this three-dimensional effect.

4.1.2. *Stationarity of the flow*

All the regimes that we described above were stationary, i.e. we always waited for several turnover times of the cylinders so that the mean positions of the menisci had become constant. Assuming the two-dimensionality of the flow, the stationary position of the menisci means that the flux of fluid is constant for all values of s. In particular:

the flux leaving the downstream meniscus in the two coating films is equal to the flux of oil which passed through the minimum gap;

the flux brought by the two coating films to the upstream meniscus is equal to the flux of oil leaving it through the minimum gap.

We will denote t_i and t_e as the thicknesses of the two films covering the inner and outer cylinders respectively. Assuming that the effect of gravity on the films is negligible, their thickness is constant and they move at the velocity of the solid surface that they cover (Moffat 1977). In this limit the flux of oil carried by the films is

$$Q = t_i V_i + t_e V_e. \tag{1}$$

The estimation of the flux of oil in the minimum gap region is more difficult. It can be easily computed only when the space between the cylinders is entirely filled. In the lubrication approximation, the surfaces being considered parabolic, the flow rate Q' is then (Savage 1977)

$$Q' = \tfrac{2}{3} b_0 (V_i + V_e). \tag{2}$$

This relation is linked with the fact that the geometry imposes a gradient of pressure between the two sides of the minimum gap so that the fluid is accelerated through it (Taylor 1963). As a result, in the minimum gap, the fluid has a velocity larger than the average velocity of the walls.

In their analysis of the position of the downstream meniscus in the printer's instability Hakim *et al.* (1990) assumed that this relation remained approximately valid in spite of the proximity of the menisci.

Equating the flux of oil carried by the films to the flux of the hydrodynamic flow in the filled region of the gap yields a relation between t_i and t_e and the ratio of the two velocities. In the particular case of perfect corotation this relation gives $t_i = t_e = 2b_0/3$.

Thus in this model, for $V_i = V_e$ the thicknesses of the films would be independent of the velocity.

But on the other hand it is well known that the thickness of a film deposited on an emerging solid surface is related to both the velocity of the surface and the thickness of the region in which the meniscus is confined, a law first derived by Bretherton (1961):

$$t \propto b(s_d)\, Ca^{2/3}, \tag{3}$$

where $b(s_d)$ is the gap thickness at the downstream meniscus position s_d and $Ca = \mu V/T$ is the capillary number. Hakim *et al.* (1990) recover their constant thickness by assuming that the downstream meniscus recedes so that in (3) the decrease of the local thickness $b(s_d)$ compensates the effect of the increase of the velocity. For exact corotation this provides an expression for the value of $b(s_d)$ and thus for the position s_d of the meniscus.

The present experiment shows that, at least in the case of filling types B and C, these assumptions are wrong. The fact that with increasing velocities both menisci recede towards the minimum gap (figure 4) means that the films become thicker. The roughest approximation in the previous calculation was the use of relation (2) which is only strictly valid in the case of an entirely filled space between the cylinders. This assumption can only retain some validity in fillings of type A.

Computations of the actual flow in a narrow gap in the presence of menisci were carried out by Gaskell *et al.* (1995) and by Reinelt (1995). The former computes the flow between two cylinders in the roll-coating geometry in the case where one thin film brings a small fixed flow of fluid into the gap. The latter revisits our experimental geometry and seeks the possible global steady regimes of the system taking into account the two menisci. He limits himself to two-dimensional situations and investigates analytically and numerically the position and stability of both menisci. In his analysis gravity is neglected and the gap is supposed to be very thin (3.3 μm on our scale) in order to remain in the low capillary number limit which is the range of validity of Bretherton's approximation (Bretherton 1961) for the thickness of the coating films. Solving the real flow of the fluid in the gap region in the presence of both menisci Reinelt deduces, as Hakim *et al.* (1990), the position of the menisci from the conservation laws. The resulting locations of the menisci are functions of the total quantity of oil that has been introduced in the cell. For both large and small quantities he observes the two menisci to recede when the velocities are increased. This demonstrates that, as in the experiment, the films do become thicker with increasing velocities. In the case of a large quantity of oil (corresponding to filling of type B in the present article) the computed evolution of the position of the menisci corresponds to our results shown on figure 4(*a*). For a smaller quantity Reinelt finds the upstream meniscus to recede so much that it passes through the minimum gap and finally settles at a positive abscissa s_u. This is exactly what we observe on figure 4(*b*) for filling of type C. In this latter case Reinelt finds that for larger velocities the upstream meniscus keeps receding but that the solution ceases to exist above a critical capillary number. If the capillary number is then decreased, the two menisci collide. At this point all the oil is spread on the surface of the cylinders and nothing is left to fill the gap. In the experiment we can observe this collision of the menisci when the total quantity of oil is even smaller than for a filling of type C or in transients following an abrupt start of the rotations.

4.2. *Nature of the instabilities*

4.2.1. *Steady and propagating waves*

We do not have an interpretation for this instability. However, a few remarks can be made.

The destabilization of the cusp between a penetrating coating film flowing into a thicker fluid layer has previously been observed (Melo & Douady 1993; Valette *et al.* 1994), but to our knowledge it never gave rise to patterns of small-amplitude waves.

If the impinging films had a modulated thickness a wavy meniscus could be observed. We thus examined the influence of gravity on the coating films. In particular the film deposited on the outer cylinder could be affected by a Rayleigh–Taylor instability while it is in an upside-down position. However comparison with the work of Limat *et al.* (1992) shows that this instability does not have time to grow in the velocity range where the waves are observed. Indeed, on carefully observing the films with tangential light no modulation of their thickness was observed.

Finally, it is well known that long-wavelength peristaltic modulations of a liquid cylinder tend to spontaneously amplify because of the Laplace law (Rayleigh 1945; Goedde & Yuen 1970). In this case the pressure due to capillary effects is larger in the thinner region so that the fluid tends to flow from these regions into the inflated ones. This process only ends when the jets breaks into drops. In the present case we have the reverse situation: a linear meniscus with a negative curvature is placed in a varying gap. If disturbed by a long-wavelength modulation, the pressure in the regions displaced towards the gap will be minimum (due to the reduction of the meniscus radius of curvature) so that the fluid will tend to flow into these zones. This provides a return force towards the linear front so that the front should be stable. In the present experiment there is an unknown mechanism by which waves are excited and sustained, which is presumably linked to a coupling of the shape of the interface with the flow in the gap.

4.2.2. *Finite-amplitude fingering instability*

The subcritical transition to a fingering instability can be intuitively understood using the results obtained in the case of depleted filling of type C. In this case, at velocities below the instability threshold, the upstream meniscus is located downstream of the minimum gap at a position $s_u > 0$ (figure 2*b*). This necessarily means that the sum of the thicknesses of the two coating films is less than the minimum gap: $t_i + t_e < b_0$. Near the instability threshold however the sum is extremely close to b_0 and a slight local disturbance is enough to make the films touch each other upstream from the minimum gap so that the front locally jumps at a position $s_{u_1} < 0$ (figure 12). In the absence of a local disturbance the same transition occurs spontaneously for a slightly larger velocity. This is due to the increase of their thickness with increasing velocity which makes the films unable to cross the minimum gap. The front which was stable at $s_u > 0$ undergoes a direct transition to a front formed of fingers at $s_{u_1} < 0$.

In order to understand the transition between these two states we must recall the results about the rate of flow in the gap separating the two cylinders. As stated above, the geometry of this gap induces a pressure gradient between the upstream and downstream sides which accelerates the flow. The strength of this effect depends on the position of the menisci and was computed by Gaskell *et al.* (1995). One of their results is that this acceleration does not exist if the two menisci are close to one another.

Returning now to our experimental situation below and above the threshold we can understand it in the following way. When both menisci are downstream (figures 2*b* and

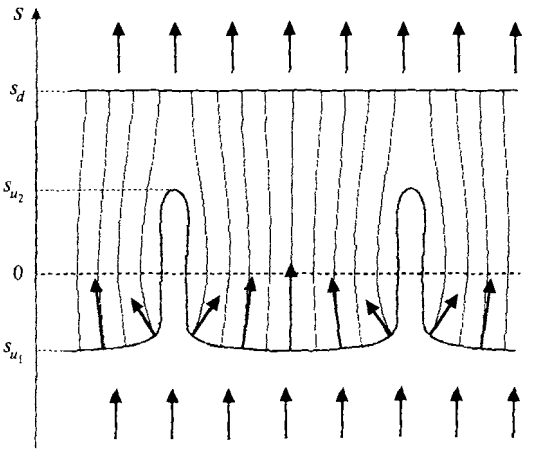

FIGURE 17. Sketch of the flow lines near the two menisci for filling C in the finger regime. The flow leaving the downstream meniscus returns to the upstream meniscus. In both the flux is constant in the spanwise direction. In contrast, in the filled region the flux is large in the fingers and zero in the air tubes.

3*b*) the flow in the filled region is slow so that the fluid brought by the films is sufficient to feed it. The two-dimensional state is thus stable. But the upstream front cannot remain at $s_u > 0$ because with increasing velocities the downstream front starts generating films that are too thick to pass through the minimum gap. As a result the upstream front has to move to $s_{u_1} < 0$ (figure 2*a*). But in this new situation the pressure gradient between the upstream and downstream sides of the gap reappears and the flow in the filled region becomes faster. The flux of oil carried away between the cylinders thus becomes larger than before, and thus larger than the flux brought by the films. The two-dimensional situation cannot be sustained. In order to solve this apparent incompatibility, the spanwise invariance is then broken and fingers are formed. In the new situation most of the front (the fingers) is located at $s_{u_1} < 0$ but the air tubes have their extremity at $s_{u_2} > 0$ (figure 17). With the presence of these tubes the conservation of the flux is recovered. The fluid is brought by the films along all the length of the meniscus. But the rate of flow between the cylinders is no longer constant in the spanwise direction. It is strong in the central region of the fingers but zero in the air tubes. This is confirmed by the observation of the trajectories of small particles present in the fluid. Figure 17 gives a qualitative sketch of the resulting flow lines.

This means that the subcritical nature of the instability in the case of filling C is a consequence of a non-local event: the existence of the topological catastrophe when the two coating films touch each other ahead of the gap.

Finally it is also possible to understand in this framework the evolution of the instability wavelength and the restabilization of the front. As the velocities are increased the films emerging from the downstream menisci have increasing thicknesses so that the influx of oil upstream increases. As a consequence it can feed the flow in a larger portion of the gap. Fewer and fewer air fingers are needed to maintain the equality of the fluxes. In the end when the influx is sufficiently large it can feed the flow along the whole length of the gap. At this point two-dimensionality becomes possible again and the front recovers its stability.

These results are compatible with the computation by Reinelt (1995) of the actual flow in the presence of menisci. He showed that filling of type C, having a stable front at $s_u > 0$, does not preclude having also $t_i + t_e < b_0$ so that the same impossibility of

maintaining a two-dimensional flow will exist in this case. However, in his article Reinelt assumed a direct relation between the limit of existence of the two-dimensional solution and the threshold of the instability. This gives threshold values V_{ic} and V_{ec} which roughly correspond to a relation of the type $V_{ic} + V_{ec} = \text{Constant}$. This is very different from the lower limit we observe (figure 5*b*). We suggest that the actual limit of stability would be obtained in Reinelt's model by plotting, in the case of filling of type C, the total thickness of the two films extracted from the downstream meniscus. Whenever this thickness exceeds that of the minimum gap, an instability would be obtained.

5. Conclusion

Directional viscous fingering (in the usual case) and Saffman–Taylor fingering are two instabilities that are directly related (Hakim *et al.* 1990). In both types of experiment, a less-viscous fluid penetrates a more-viscous fluid and the destabilizing factor is the contrast in viscosity (Saffman & Taylor 1958). In Saffman–Taylor fingering there is only one stabilizing factor: the surface tension which can only act for short wavelengths. For this reason the Saffman–Taylor instability has no threshold and no bound to its growth. In contrast, in the usual directional viscous fingering there are two stabilizing factors: the surface tension at small scales and the thickness gradient at large scales. As a result there is a finite threshold to the printer's instability. Above this threshold the thickness gradient still acts on the front as a return force so that the amplitude of the fingers is limited by nonlinear terms.

In the present article we have examined the stability of the upstream front where the direction of the flow is opposite. In this situation the effect of the viscosity contrast becomes a stabilizing factor and surface tension remains stabilizing. It is now the thickness gradient which becomes the destabilizing factor; we believe it is the origin of the instability that we have described.

We thank Vahé Ter Minassian and Michel Decré for their help during this experiment, and D. A. Reinelt for sending us his preprint prior to publication.

REFERENCES

BRATTKUS, K. 1989 Capillary instabilities in deep cells during directional solidification. *J. Phys. Paris* **50**, 2999–3006.

BRETHERTON, F. P. 1961 The motion of long bubbles in tubes. *J. Fluid Mech.* **10**, 166–188.

COULLET, P. & IOOSS, G. 1990 Instabilities of one-dimensional cellular patterns. *Phys. Rev. Lett.* **64**, 866–869.

CROSS, M. C. & HOHENBERG, P. C. 1993 Pattern formation outside equilibrium. *Rev. Mod. Phys.* **65**, 851–1112.

CUMMINS, H. Z., FOURTUNE, L. & RABAUD, M. 1993 Successive bifurcations in directional viscous fingering. *Phys. Rev.* E **47**, 1727–1738.

DAVIAUD, F., BONNETTI, M. & DUBOIS, M. 1990 Transition to turbulence via spatiotemporal intermittency in one-dimensional Rayleigh–Bénard convection. *Phys. Rev.* A **42**, 3388–3399.

DECRÉ, M. 1994 Etude expérimentale des comportements de l'interface dans l'enduisage par rouleaux. Thèse de l'Université Paris VI.

DOUADY, S., FAUVE, S. & THUAL, O. 1989 Oscillatory phase modulation of parametrically forced surface waves. *Europhys. Lett.* **10**, 309–315.

FAIVRE, G., DE CHEVEIGNÉ, S., GUTHMANN, C. & KUROWSKI, P. 1989 Solitary tilt waves in thin lamellar eutectics. *Europhys. Lett.* **9**, 779–784.

FLESSELLES, J.-M., SIMON, A. J. & LIBCHABER, A. J. 1991 Dynamics of one-dimensional interfaces: an experimentalist's view. *Adv. Phys.* **40**, 1–51.

GASKELL, P. H., SAVAGE, M. D., SUMMERS, J. L. & THOMPSON, H. M. 1995 Modelling and analysis of meniscus coating. *J. Fluid Mech.* **298**, 113–137.

GOEDDE, E. F. & YUEN, M. C. 1970 Experiments on liquid jet instability. *J. Fluid Mech.* **40**, 495–511.

HAKIM, V., RABAUD, M., THOMÉ, H. & COUDER, Y. 1990 Directional growth in viscous fingering. In *New trends in Nonlinear Dynamics and Pattern Forming Phenomena* (ed. P. Coullet & P. Huerre), pp. 327–337. Plenum.

JACKSON, K. A. & HUNT, J. D. 1965 Transparent compounds that freeze like metals. *Acta Metall.* **13**, 1212–1215.

KUROWSKI, P., DE CHEVEIGNÉ, S., FAIVRE, G. & GUTHMANN, C. 1989 Cusp instability in cellular growth. *J. Phys. Paris* **50**, 3007–3019.

KUROWSKI, P., DE CHEVEIGNÉ, S. & GUTHMANN, C. 1990 Shapes, wavelength-selection, and the cellular-dendritic "transition" in directional solidification. *Phys. Rev.* A **42**, 7368–7376.

LIMAT, L., JENFFER, P., DAGENS, B., TOURON, E., FERMIGIER, M. & WESFREID, J. E. 1992 Gravitational instabilities of thin liquid layers: dynamics of pattern selection. *Physica* D **61**, 166–182.

MELO, F. & DOUADY, S. 1993 From solitary waves to static patterns via spatiotemporal intermittency. *Phys. Rev. Lett.* **71**, 3283–3286.

MICHALLAND, S. 1992 Etude des différents régimes dynamiques de l'instabilité de l'imprimeur. Thèse de l'Université Paris VI.

MICHALLAND, S., RABAUD, M. & COUDER, Y. 1993 Transition to chaos by spatio-temporal intermittency in directional viscous fingering. *Europhys. Lett.* **22**, 17–22.

MOFFATT, H. K. 1977 Behaviour of a viscous film on the outer surface of a rotating cylinder. *J. Méc.* **16**, 651–673.

OSWALD, P., BECHHOEFFER, J. & LIBCHABER, A. 1987 Instabilities of a moving nematic-isotropic interface. *Phys. Rev. Lett.* **58**, 2318–2321.

PAN, L. & DE BRUYN, J. R. 1993 Spatially uniform travelling cellular patterns at a driven interface. *Phys. Rev.* E **49**, 483–493.

RABAUD, M., COUDER, Y. & MICHALLAND, S. 1991 Wavelength selection and transients in the one-dimensional array of cells of the printer's instability. *Euro. J. Mech.* B/*Fluids* **10**, 253–260.

RABAUD, M., MICHALLAND, S. & COUDER, Y. 1990 Dynamical regimes of directional viscous fingering: spatiotemporal chaos and wave propagation. *Phys. Rev. Lett.* **64**, 184–187.

RAYLEIGH, LORD 1945 *Hydrodynamics* (6th edn). Dover.

REINELT, D. A. 1995 The primary and the inverse instabilities of directional viscous fingering. *J. Fluid Mech.* **285**, 303–327.

SAFFMAN, P. G. & TAYLOR, G. I. 1958 The penetration of a fluid into a porous medium or Hele–Shaw cell containing a more viscous liquid. *Proc. R. Soc. Lond.* A **245**, 312–329.

SAVAGE, M. D. 1977 Cavitation in lubrication. Part 1. On boundary conditions and cavity-fluid interfaces. *J. Fluid Mech.* **80**, 743–755.

SIMON, A. J. & LIBCHABER, A. 1990 Moving interface: the stability tongue and phenomena within *Phys. Rev.* A **41**, 7090–7093.

TAYLOR, G. I. 1963 Cavitation of a viscous fluid in narrow passages. *J. Fluid Mech.* **16**, 595–619.

VALETTE, D. P., EDWARDS, W. S. & GOLLUB, J. P. 1994 Transition to spatiotemporal chaos via spatially subharmonic oscillations of a periodic front. *Phys. Rev.* E **49**, R4783–R4786.